Sensor and Simulation Notes

Note 327

27 April 1991

# Configurations of TEM Feed for an IRA

Carl E. Baum

Phillips Laboratory
Kirtland Air Force Base
Albuquerque, NM 87117

## Abstract

paper considers some of the design options for an antenna consisting of a parabolic ector with a terminated TEM feed. With a fast-rising (step-like) source, this gives an oximate impulse radiating antenna (IRA). Design options include cable networks for ing the TEM feed, including dual polarization. Adjustment of the feed-termination edance at low frequencies can balance the electric- and magnetic-dipole moments. cial media near the feed apex can aide in launching fast, high-voltage pulses in the TEM le.

WL-EMP-SSN-327

Sensor and Simulation Notes

Note 327

27 April 1991

# Configurations of TEM Feed for an IRA

Carl E. Baum

Phillips Laboratory
Kirtland Air Force Base
Albuquerque, NM 87117

## Abstract

This paper considers some of the design options for an antenna consisting of a parabolic reflector with a terminated TEM feed. With a fast-rising (step-like) source, this gives an approximate impulse radiating antenna (IRA). Design options include cable networks for driving the TEM feed, including dual polarization. Adjustment of the feed-termination impedance at low frequencies can balance the electric- and magnetic-dipole moments. Special media near the feed apex can aide in launching fast, high-voltage pulses in the TEM mode.

TEM waves, impulse radiating antenna (IRA)

## I. Introduction

The basic concept of an IRA (impulse radiating antenna) is as described in [15]. It is more than a spherical TEM wave (non-dispersive) feeding a parabolic reflector [21], as it includes a termination of the TEM transmission line so that the transient radiated waveform does not include unwanted reflections on the antenna feed, but approximates an impulse within the constraints of a finite size driven by a fast-rising finite energy source. This termination also influences the low-frequency radiation by giving both electric- and magnetic-dipole moments which give a radiation pattern peaking in roughly the same direction as the high-frequency reflector pattern (or precisely the same pattern peak for symmetric reflector and feed). The resulting waveform has some aspects associated with the reflector (impulse part), the feed (step part), and combinations of the two ($\vec{p} \times \vec{m}$ part).

This paper explores some of the possibilities for the TEM feed, in terms of geometry, impedances, and electrical networks for driving the feed. This involves the topology of cable and signal sources, symmetry in the antenna/feed, and special considerations near the feed apex and termination locations.

## II. Some Feed-Network Options

As discussed in [15] we have the example of a single TEM feed, perhaps with an offset feed for beam steering and/or reduction of feed blockage. Staying with this context for the moment, consider some of the possibilities. As in Figure 2.1 consider some of the simple possibilities for driving the TEM feed. One might use charge lines (or capacitors) on each feed arm with a switch at the apex (Figure 2.1A). Thereby a high voltage, fast-rising wave can be launched. With high-resistance connections to power supplies one can avoid shorting out the terminations to the reflector. An alternate approach involves high quality coaxes made part of the feed conical conductors transmitting fast-rising pulses to the feed conical apex (Figure 2.1B). In this case one might use high-quality inductive chokes to avoid having the cable shields affect the terminations. Note that several kinds of signal connections at the feed apex are possible (Figure 2.1C), including single ended (for single coaxes or charge lines) and split shield or Moebius for differential systems [1,2]. Switches can be included as part of these connections as desired.

Still sticking with single TEM feeds Figure 2.2 shows that symmetry can be used if the reflector and feed have a common symmetry plane P. In this case the fields are antisymmetric with respect to P [16] which can now accommodate a highly conducting sheet or other approximately planar assemblage of conductors (e.g. coaxial cables). Furthermore one can use this symmetry plane to mount half of the reflector/feed system on a ground plane for various experimental purposes. As indicated in Figure 2.3 one can now use the symmetry plane to accommodate charge lines and coaxial cables instead of running them along the conical feed arms as in Figure 2.1, thereby avoiding the problem of running cables in parallel with the feed-termination impedances. Figure 2.3A shows cables on the symmetry plane coming from below the reflector. In Figure 2.3B the cables come from the center of the reflector allowing one to construct movable cable bends (if desired) which can be combined with pivots at the TEM feed terminations to permit movement of the feed to scan the reflector beam (in a direction along P). Figure 2.3C shows that a single coaxial cable can be used (in both previous examples) by use of a single-ended-to-differential balun.

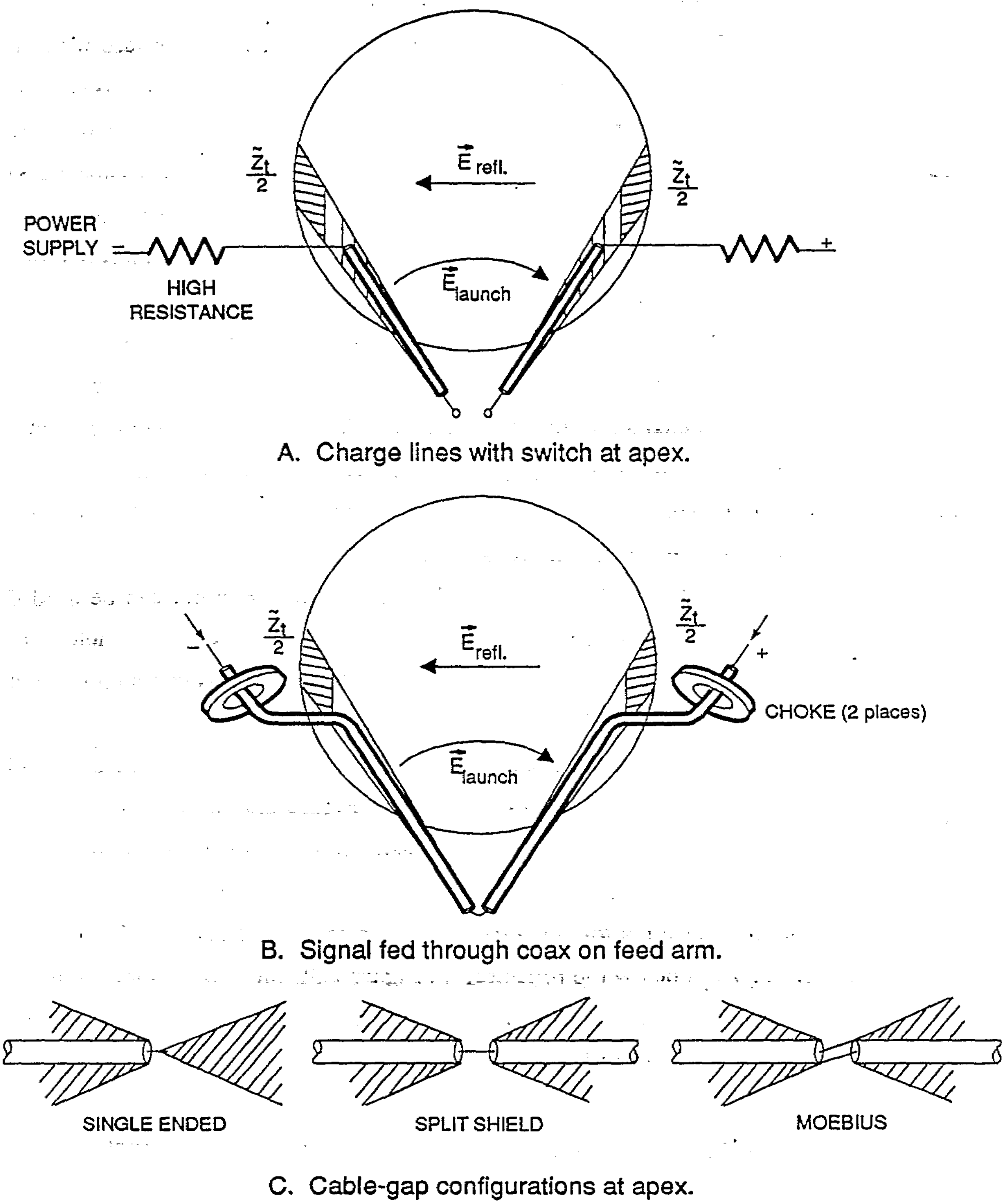


**Figure 2.1. Feeding Conical Apex**

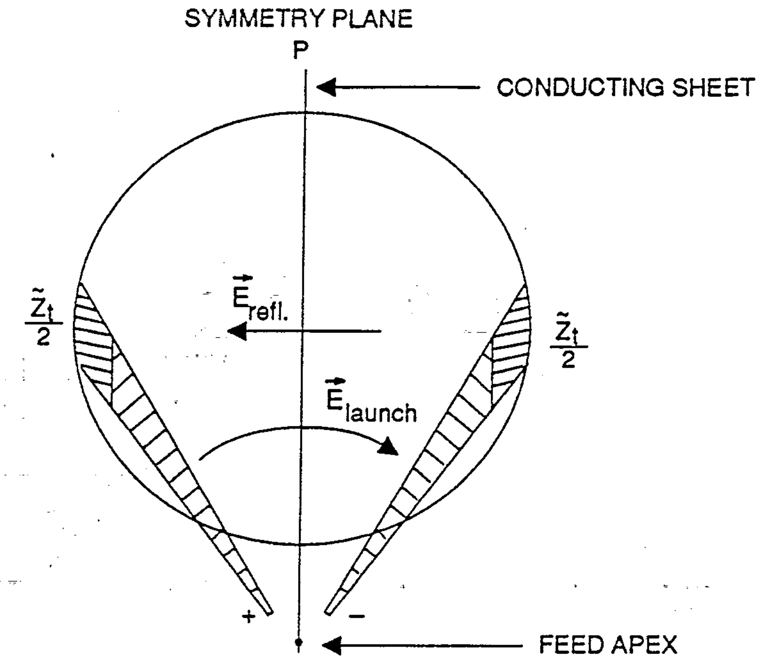


A. Front view

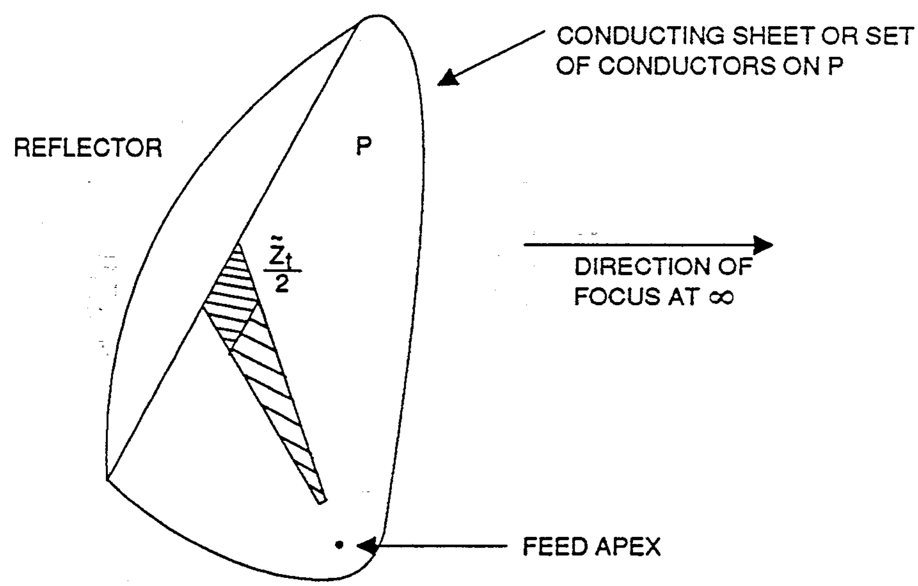


B. Side view

**Figure 2.2. Conductors on Symmetry Plane**

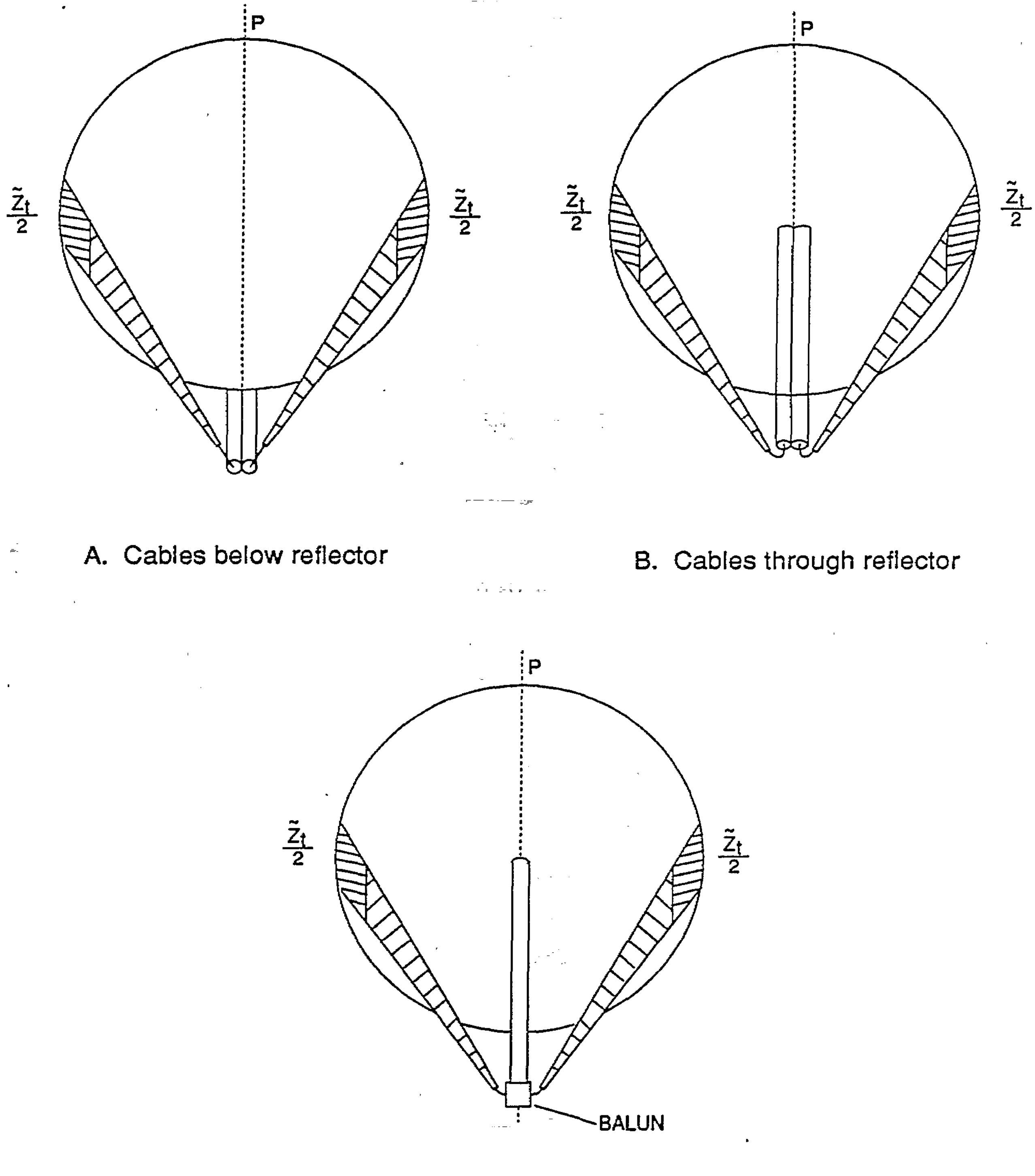


A. Cables below reflector

B. Cables through reflector

C. Single cable with balun

**Figure 2.3. Signal Cables on Symmetry Plane**

## III. Dual-Polarization Geometries

So far our examples have been for a single TEM feed. Consider now the case that we have two such feeds which can launch independent TEM waves toward the reflector. For simplicity let the reflector/feed system have $C_{4a}$ symmetry [20], a 4-fold rotation axis with axial symmetry planes labeled as $P_1$ through $P_4$ in Figure 3.1. One can also label the feed arms 1 through 4 according to the voltages $V_1$ through $V_4$, as indicated. Considering feed arms 1 and 2 centered on $P_1$ one can set $V_2 = -V_1$ with $V_2 = V_4 = 0$ to launch a horizontal (parallel to $P_1$) electric field. Similarly driving between arms 2 and 4 launches a vertical (parallel to $P_3$) electric field.

As indicated in Figure 3.1A the feed arms (conical plates) are oriented so that they approximately match the reflector edge. When the wave reflects from the parabolic reflector it interacts with the feed structure (feed blockage and scattering). In the high-frequency ($s \to \infty$) or early-time limit one can estimate the blockage of the main beam from optical considerations, basically removing the rays that are intercepted by the feed structure. As indicated in Figure 3.1B one can rotate the feed arms so that they are parallel to (coincide with) $P_1$ and $P_3$. From an optical point of view this mostly eliminates the feed blockage, but as frequency is decreased so that wavelengths are of the order of the width of the plates (or larger), the reorientation of the plates is less significant. One could also use circular-conical conductors if preferred for some reason.

The side views show a typical reflector geometry adapted to the TEM feed. The conical-transmission-line apex is at the reflector focus, a distance F from the reflector center. With the reflector diameter D, we have a typical F/D of around 0.4 for typical antenna designs. Whether this ratio is optimal for our purposes is a matter for further investigation. The width (or better angular width) of the conical plates is another variable of concern. Let $Z_1$ be the characteristic impedance of each feed for $P_1$ or $P_3$ polarization with face-on plates as in Figure 3.1A. As calculated in [6,7] we have $Z_1$ as a function of the plate width 2a, plate separation 2b and length of line $\ell$. For say $b/a \approx 7$ we have $Z_1 = 400\Omega$. For smaller $b/a$ of order 1 this impedance can be lowered to say $200\Omega$, but this gives very wide plates and lots of reflector blockage. So let us assume for present convenience a $Z_1$ of $400\Omega$. Note that if the plates are rotated to edge-on configuration as in Figure 3.1B the impedance will be roughly the same. One can make an accurate calculation using the

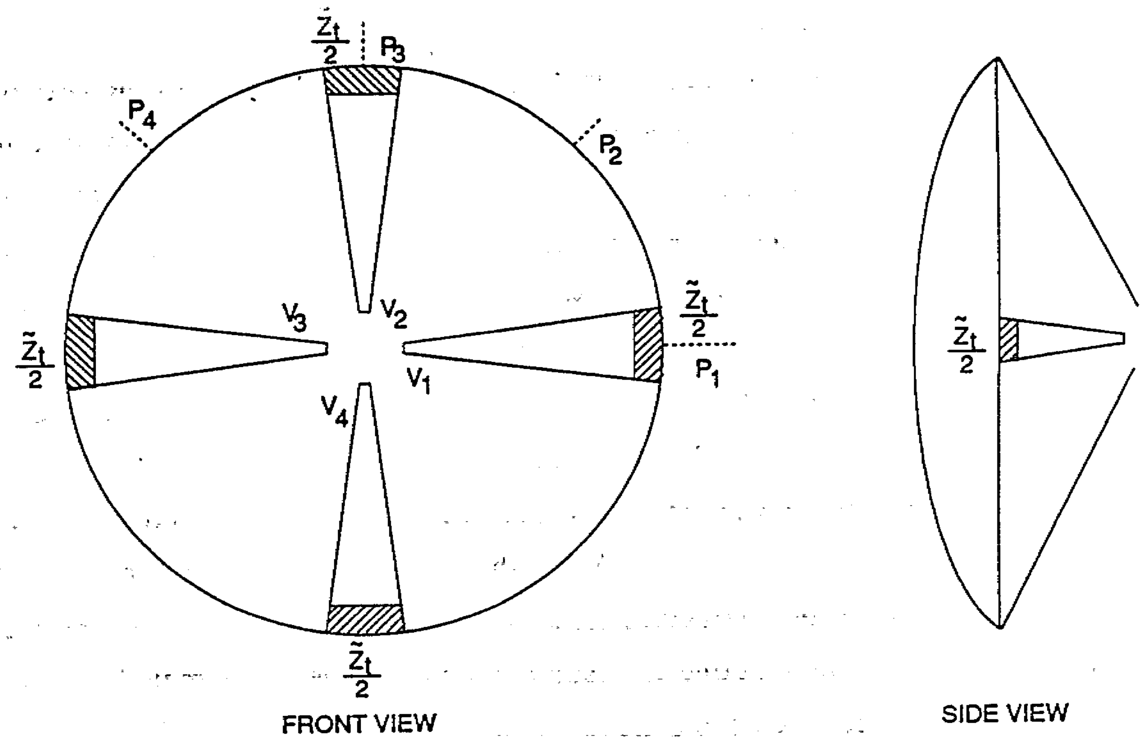


A. Face - on feed arms

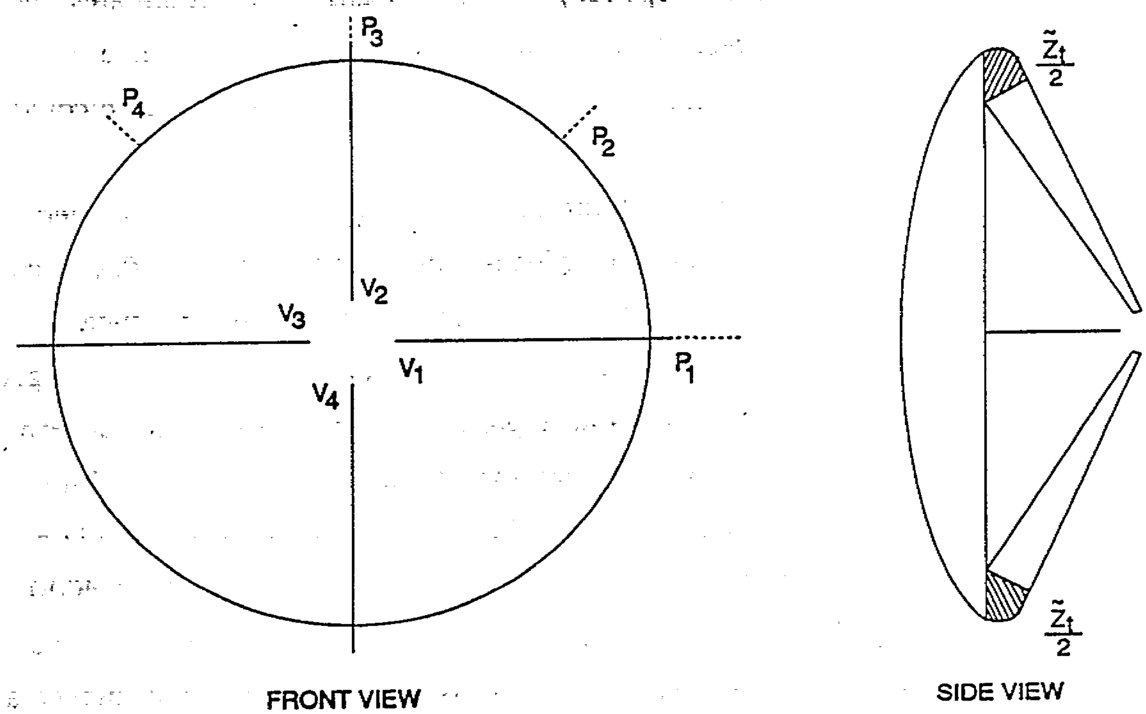


B. Edge - on feed arms

**Figure 3.1. Dual Polarization Feeds with $C_{4a}$ Symmetry**

combination of stereographic projection and conformal transformation as in [4] where now the conformal transformation is for coplanar strips. Furthermore, this case has the plates on $P_3$ not affecting the calculation of the impedance for $P_1$ plates, being orthogonal to the electric field.

With the $C_{4a}$ antenna symmetry in Figure 3.1 (with either orientation of feed plates, or even other shapes such as circular cones) consider driving the field parallel to $P_1$. This case has

$$V_1 = -V_3 = V \ , \ I_1 = -I_3 = 0$$

$$V_2 = V_4 = O \ , \ I_2 = I_4 = O \tag{3.1}$$

$$Z_1 \equiv \frac{V_1 - V_3}{I_1} = \frac{2V}{I}$$

where current convention is taken as positive into the feed arms. By symmetry if we drive the field parallel to $P_3$ we obtain the same impedance, say $400\Omega$ in each case. Since the symmetry (orthogonality) of the two configurations allows us to drive both ways independently (without mutual interaction) consider the case in which we drive both equally (electrically in parallel) as

$$V_1 = V_2 = -V_3 = -V_4 = V$$

$$I_1 = I_2 = -I_3 = -I_4 = I$$

$$Z_2 \equiv \frac{V_1 - V_3}{I_1 + I_2} = \frac{V_2 - V_4}{I_1 + I_2} = \frac{2V}{2I} = \frac{V}{I} \tag{3.2}$$

$$Z_2 = \frac{Z_1}{2}$$

The radiated fields contribute equally (at right angles) on the symmetry axis giving a field polarized parallel to $P_2$. Furthermore the impedance is cut in half, to say $200\Omega$.

Thus connecting arms 1 to 2 and 3 to 4 gives $P_2$ polarization. Similarly connecting arms 2 to 3 and 1 to 4 gives the orthogonal polarization, i.e. parallel to $P_4$. However, one can completely analyze or measure the antenna performance by considering $P_1$ or $P_3$ polarization (both being the same by a $\pi/2$ rotation). One can then replace one of the symmetry planes, say $P_1$, by a conducting plane and drive arm 2 to completely experimentally characterize the antenna.

## IV. Some More Elaborate Feed-Options Involving Cable Topology

Section II shows some ways to configure signal cables and charge lines (or capacitors) to drive a single TEM feed, either along the feed arms with due regard to not interfering with the feed terminations, or (perhaps with additional conductors) along a symmetry plane between the feed arms. In Section III the use of two TEM feeds was introduced. Each feed can be driven by the same techniques noting that cables on the original symmetry plane are now restricted to the symmetry axis (so as to interfere with neither feed). Such techniques can be applied to cases involving $P_1$ and $P_3$ polarization, or $P_2$ and $P_4$ polarization. In the latter case one can use a rotating switch at the mutual conical apex or special transformers (with due consideration to bandwidth) to achieve both polarizations.

An increased flexibility is obtained by using both feed arms and symmetry axis for routing cables. Figure 4.1 shows two examples of cable networks using this added flexibility. Figure 4.1A diagrams a case where the feed characteristic impedance is assumed to be $400\Omega$, appropriate to $P_1$ and $P_3$ polarization in Figure 3.1. In this case, say for $P_1$ polarization, $200\Omega$ coaxial cables are made parts of arms 1 and 3 with two such cables along the symmetry axis. With $200\Omega$ for each half of the reflector, a differential pair of such cables join in a split-shield gap near the feed apex. Behind the reflector + cables and - cables are separately joined (with identical transit times to feed apex) in parallel into separate $50\Omega$ cables. The + and - $50\Omega$ cables form a $100\Omega$ differential drive. A similar $100\Omega$ differential system can drive (or receive) for $P_3$ polarization. Note the chokes on the cables passing over terminations.

Figure 4.1B diagrams a case where the feed impedance is taken as $200\Omega$, appropriate to $P_2$ and $P_4$ polarization as discussed in Section III. In this case let $100\Omega$ cables be parts of, say, arm 2 and the conductor bundle on the symmetry axis. With $100\Omega$ for each half of the reflector, there are two single ended gaps near the feed apex. Behind the reflector the two cables (same polarity, say +) are joined (with identical transit times to feed apex) in parallel into a single $50\Omega$ cable, a single-ended system. By connecting arms in pairs near the feed apex (as discussed in Section III) one can produce $P_2$ and $P_4$ polarization (separately). One can also place another such cable network (say on arm 1 and the symmetry axis) and use special transformers near the feed axis to operate both polarizations simultaneously.

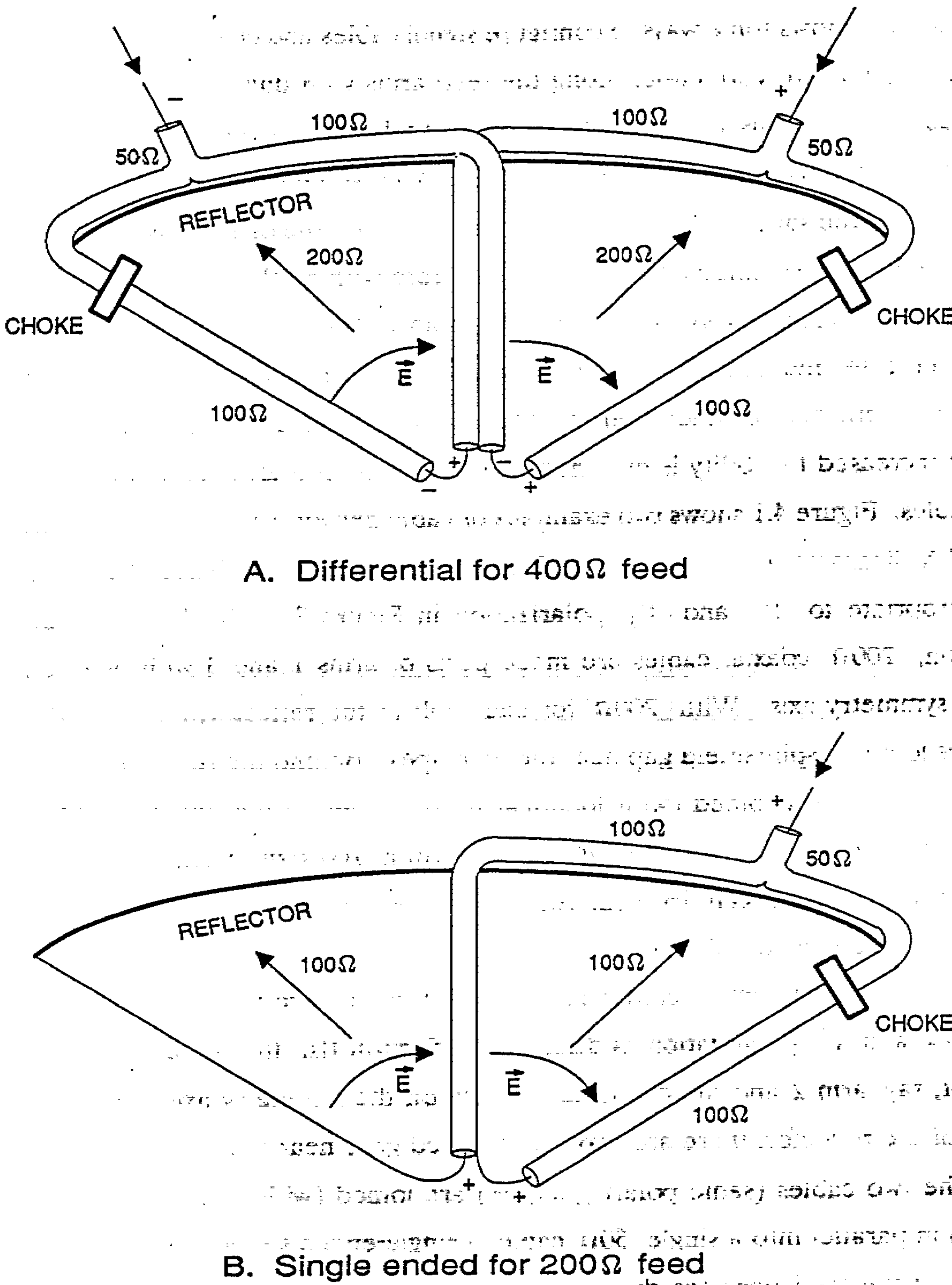


**Figure 4.1. Cable Topologies for Antenna Feed**

These examples show some of the possibilities for such cable-feed networks. More elaborate cable topologies are also possible using some of the concepts for loop sensors [2,3,18,19].

## V. $\vec{p} \times \vec{m}$ Antenna at Low Frequencies

As discussed in [15] an IRA has its low frequency behavior dominated by electric- and magnetic-dipole moments which re-enforce in the main reflector-beam direction. For the symmetrical feed geometries in Section III, this is exactly the case with $\vec{p} \times \vec{m}$ along the symmetry axis. If we can balance these as

$$\vec{p} = p\,\vec{1}_p\,,\ \vec{m} = m\,\vec{1}_m\,,\ p = \frac{m}{c}$$

$$\vec{1}_p \times \vec{1}_m = \vec{1}_2 \tag{5.1}$$

then the dipole terms $(r^{-1}, r^{-2}, r^{-3})$ give electric and magnetic fields related as $Z_0$ (377Ω) in the forward direction, with only an $r^{-3}$ term in the back direction [5,8]. There are ways to design an antenna with this special balanced property [8,14]. Perhaps this can be accomplished in the present case as well.

As discussed in [8,14] one can produce this special low-frequency property by driving a terminated TEM transmission line. However, the approach involves small plate-spacing-to-length ratios for the simple per-unit-length considerations to apply. For the IRA concept discussed here we have a TEM-transmission-line feed, but as in Figure 3.1 the plate "spacing" may be greater than the length. Furthermore the reflector, while closing the current loop, is at zero potential relative to the feed arms, giving an undesired low-frequency charge on the reflector.

However, one can adjust the ratio of the charge (for $\vec{p}$) to the current (for $\vec{m}$) by adjusting $\tilde{Z}_t$ at low frequencies. For frequencies corresponding to wavelengths of the order of the feed length, $\tilde{Z}_t$ should approximate the resistive $\tilde{Z}_1$ (Section III). For frequencies such that the feed length is electrically short $\tilde{Z}_t$ can be made resistive, but greater than $\tilde{Z}_1$. The particular value to be used depends on that required to achieve the balance in (5.1). When this balance is achieved then the low-frequency radiation has a null behind the reflector (on the symmetry axis), and this null can be used as an experimental way to determine the required termination resistance.

## VI. Considerations for High Electric Fields Near Feed Apex

As one goes to higher and higher voltage pulses launched onto the TEM feed one eventually encounters electrical breakdown near the feed apex. As one goes to faster and faster risetimes one needs to establish the TEM mode field distribution over the cross section of the feed at positions close enough to the apex that such a risetime for the fields can be effectively constructed over the entire cross section. While the conical feed can be thought of as a transmission line, it is more than that. It is a waveguide which can support higher order modes besides the TEM mode. For present purposes we would like to have only the non-dispersive TEM mode with a fast risetime, and suppress the unwanted higher order modes.

Using concepts similar to those for EMP simulators one starts with the desired TEM mode at some radial distance from the apex where the fields are small enough (say in 1 atmosphere air). Then work backwards toward the apex until one arrives at a position where the electric field is large enough that something needs to be done, while not significantly distorting the TEM mode. Then keep going until something else needs to be done, etc.

Figure 6.1, shows some of the things that can be done. Going back toward the apex one might first construct a gas enclosure holding 1 atmosphere (absolute pressure) of a high-dielectric-strength gas such as $SF_6$ . With no significant pressure differential (gauge pressure) the enclosure can be made of a thin dielectric which will not significantly perturb the wave. Note that the conical conductors pass through the enclosure wall (with a gas seal). This front wall, through which the most significant part of the TEM mode passes, requires the greatest attention to minimize interference with the TEM mode. Having passed through the dielectric membrane on the way toward the apex, the conical conductors are extended toward smaller cross section until the electric field is large enough that something else needs to be done. As indicated in Figure 6.1 this could be another gas enclosure, this time pressurized to further increase the breakdown strength. Now the enclosure needs to be structurally stronger (but fortunately at a smaller size), giving thicker dielectric walls for careful treatment on the front wall where the conical conductors again penetrate.

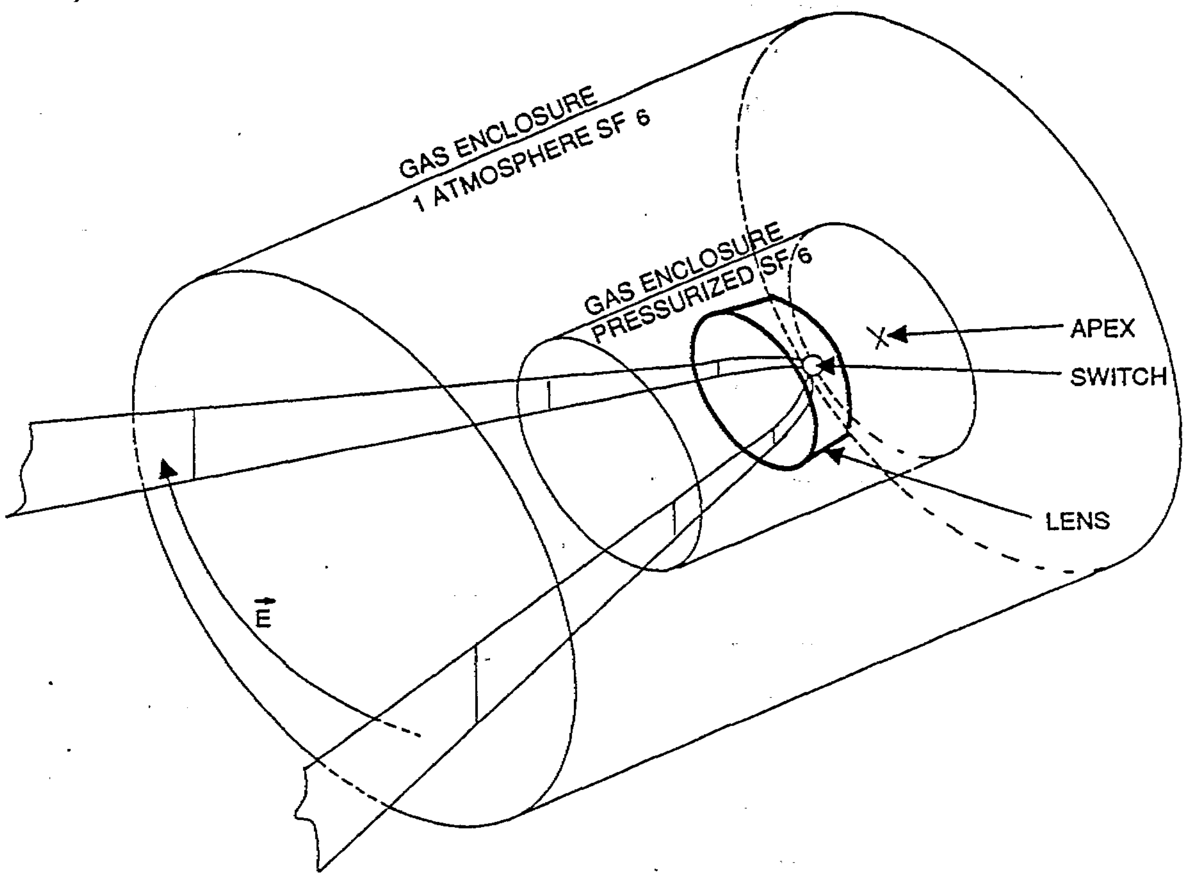


**Figure 6.1. Design for High Voltages Near Feed Apex**

Going into the pressurized gas the conical conductors go even closer together until the electric field approaches breakdown. Now one may introduce a transient lens [22]. This lens needs a high dielectric strength (such as transformer oil, solid dielectrics, etc.) in combination with the basic electromagnetic properties of the lens. The function of the lens is to transition from the conical TEM wave back to yet smaller dimensions (and even higher electric fields) where the wave is originated by say a switch (or spark gap) or array of such switches. The lens may be rather complex in shape and constituents since its purpose is to move the wave around in space in such a way that it matches to the desired TEM mode at the front face of the lens without dispersion, reflections, etc.

The switch can also be constructed as an array of switches using the distributed-switch concept [9]. Here the desired tangential electric fields are synthesized on a surface in time, vector orientation, and vector magnitude. This is an approximate realization in that the surface is broken into smaller patches, each patch having a source (switch) which is appropriately connected to adjacent patches and triggered at the correct time. There are various ways to improve the performance for each patch by special wave launchers combined with each switch [10,11,12,13,17]. One might even incorporate a transient lens in each patch wave launcher. Note now that switch jitter is important in that it limits the wave synthesis in a time sense.

One might not use all the techniques in Figure 6.1 for a particular design. This involves the EM performance quality attainable in the various components and the risetime and voltages desired.

## VII. Concluding Remarks

As we can now see there are many design features for an IRA. These concern shapes of the TEM feed arms. Cable networks and switch configurations come in several varieties for feeding the antenna. The feed terminations can be used to improve the low-frequency performance in a $\vec{p} \times \vec{m}$ directional sense. The feed can be made to support fast risetimes with high voltages using special insulation techniques which are consistent with the desired TEM mode.

There are still some design variations to be considered. One can vary the feed geometry along the feed to compromise between the ideal TEM modal structure and the aperture blockage. There is also the question of sidelobe suppression, perhaps using strategically placed absorber materials near the reflector outer edge and/or on the feed arms near the reflector.

## References


1. C. E. Baum, Characteristics of the Moebius Strip Loop, Sensor and Simulation Note 7, December 1964.

2. C. E. Baum, A Technique for the Distribution of Signal Inputs to Loops, Sensor and Simulation Note 23, July 1966.

3. C. E. Baum, the Multiple Moebius Strip Loop, Sensor and Simulation Note 25, August 1966.

4. C. E. Baum, A Conical-Transmission-Line Gap for a Cylindrical Loop, Sensor and Simulation Note 42, May 1967.

5. C. E. Baum, Some Characteristics of Electric and Magnetic Dipole Antennas for Radiating Transient Pulses, Sensor and Simulation Note 125, January 1971.

6. F. C. Yang and K. S. H. Lee, Impedance of a Two-Conical-Plate Transmission Line, Sensor and Simulation Note 221, November 1976.

7. F. C. Yang and L. Marin, Field Distribution on a Two-Conical-Plate and a Curved Cylindrical-Plate Transmission Line, Sensor and Simulation Note 229, September 1977.

8. J. S. Yu, C-L.J. Chen, and C. E. Baum, Multipole Radiations: Formulation and Evaluation for Small EMP Simulators, Sensor and Simulation Note 243, July 1978.

9. C. E. Baum and D. V. Giri, The Distributed Switch for Launching Spherical Waves, Sensor and Simulation Note 289, August 1985, and Proc. EMC Symposium, Zurich, March 1987, pp. 205-212.

10. C. E. Baum, Coupled Transmission-Line Model of Periodic Array of Wave Launchers, Sensor and Simulation Note 313, December 1988.

11. D. V. Giri, Impedance Matrix Characterization of an Incremental Length of a Periodic Array of Wave Launchers, Sensor and Simulation Note 316, April 1989.

12. C. E. Baum, Canonical Examples for High-Frequency Propagation on Unit Cell of Wave-Launcher Array, Sensor and Simulation Note 317, April 1989.

13. D. V. Giri, A Family of Canonical Examples for High Frequency Propagation on Unit Cell of Wave-Launcher Array, Sensor and Simulation Note 318, June 1989.

14. E. G. Farr and J. S. Hostra, An Incident Field Sensor for EMP Measurements, Sensor and Simulation Note 319, November 1989, and IEEE Trans. EMC, 1991, pp. 105-112.

15. C. E. Baum, Radiation of Impulse-Like Transient Fields, Sensor and Simulation Note 321, November 1989.

16. C. E. Baum, Interaction of Electromagnetic Fields With an Object Which has an Electromagnetic Symmetry Plane, Interaction Note 63, March 1971.

17. J. Nitsch, C. E. Baum, and R. Sturm, The Treatment of Commuting Nonuniform Tubes in Multiconductor-Transmission-Line Theory, Interaction Note 481, May 1990.

18. C. E. Baum, Winding Topology for Transformers, Measurement Note 31, October 1986.

19. C. E. Baum, Winding Bundles for Transformers, Measurement Note 35, November 1987.

20. C. E. Baum and H. N. Kritikos, Symmetry in Electromagnetics, Physics Note 2, December 1990.

21. H. E. King and J. L. Wong, Measured RF Characteristics of a TEM-Wire Fed Reflector, 1990 IEEE Antennas and Propagation Symposium Digest, Vol. I, pp. 266-269.

22. C. E. Baum and A. P. Stone, Transient Lens Synthesis: Differential Geometry in Electromagnetic Theory, Hemisphere Publishing Corp., New York, 1991.